ORIGINAL PAPER

Electrochemical noise analysis on the crevice corrosion behavior of Ni–Cr–Mo–V high strength steel using recurrence plots

**Tao Zhang · Yuan Cong · Yawei Shao ·
Guozhe Meng · Fuhui Wang**

Abstract This article makes a study of electrochemical noise analysis on the crevice corrosion behavior of Ni–Cr–Mo–V high strength steel using recurrence plots. The crevice corrosion behavior of Ni–Cr–Mo–V high strength steel was investigated by the electrochemical noise (EN) technique and SEM observation. The experimental results reveal that the crevice corrosion could be distinguished by three stages including induction stage, transformation stage, and stable stage. While increasing the growth probability of metastable corrosion, the presence of crevice decreases the initiation rate of metastable corrosion. In the case of crevice, the metastable corrosion is easy to develop into stable one.

Keywords Crevice corrosion · Electrochemical noise · Recurrence plots · High strength steel

1 Introduction

Crevice corrosion is still a very dangerous type of localized corrosion and commonly occurs on passive materials. Inside small crevices, the electrolyte exchange is severely disabled and, therefore, the corrosion condition can be aggravating over time [1, 2]. In the last several decades, crevice corrosion was a hot topic for many scientists. Some methods have been proposed to study the mechanism of crevice corrosion including simulation of the crevice structure and the occluded environment [3], studying the changes in the chemical composition of the occluded solution [4] and measurement of the potential distribution inside the crevice by combination electrode [5] or multiple electrodes arranged linearly inside the crevice [6]. Briefly, two mechanisms exist for crevice corrosion: a chemical transformation mechanism [1, 7, 8] and an IR drop mechanism [9–14].

Electrochemical noise (EN) gained popularity in the recent years and has emerged as a promising technology for corrosion analysis. EN shows some advantages compared to the common electrochemical techniques: first, EN is able to instantaneously monitor the rate of the corrosion process [15–20]; second, EN is carried out without artificial disturbance of the system [15–20]; last, EN can provide more information of localized corrosion than conventional techniques [21–32].

Some researchers pointed out that EN signals show chaos nature and the geometry of the dynamics exploiting non-linear dependencies even in non-stationary time series [33–36]. Recurrence plots analysis is new approach to study the behavior of non-linear dynamical systems [33–36].

As reviewed above, in the present work, recurrence plots applied to electrochemical current noise signals have been used to assess changes in the dynamics of the crevice corrosion process on Ni–Cr–Mo–V high strength steel exposed to sodium chloride aqueous solution.

2 Experimental

2.1 Materials

An artificial crevice was constructed according to ASTM standard G 48-97 [37], a plexiglas sheet of about 5 mm

T. Zhang (✉) · Y. Cong · Y. Shao · G. Meng · F. Wang
Corrosion and Protection Laboratory, Key Laboratory of Superlight Materials and Surface Technology (Harbin Engineering University), Ministry of Education,
145 Nantong Street, Harbin 150001, China
e-mail: zhangtao@hrbeu.edu.cn

T. Zhang · Y. Shao · G. Meng · F. Wang
State Key Laboratory for Corrosion and Protection,
Institute of Metal Research, Chinese Academy of Sciences,
62 Wencui Road, Shenyang 110016, China

thickness was attached to the electrode surface to form a crevice between plexiglas sheet and electrode surface (Fig. 1). The crevice gap is about 20 μm.

The investigated material was a hot rolled plate of Ni–Cr–Mo–V steel (nominal composition (wt%): C 0.1, Si 0.21, Mn 0.56, Ni 4.48, Cr 0.56, Mo 0.51, V 0.007, S 0.005, P 0.011, and Fe balance). The dimension of the specimen was 10 mm × 10 mm × 10 mm which was mounted in epoxy resin with an exposed area of 1 cm^2. All specimens were wet ground to a 2000 grit-finish, cleansed with distilled water and dried in a compressed hot air. The microstructure of Ni–Cr–Mo–V steel was characterized by laminar martensite with different orientations (Fig. 2).

2.2 Electrochemical measurements

Polarization curve was performed in a three-electrode cell, using a platinum sized 20 mm × 20 mm as counter electrode and an Ag/AgCl (saturated KCl) electrode as reference electrode. The polarization curves were measured with the scan rate of 0.333 mV/s. And the electrochemical measurements were carried out in 3.5% NaCl solution at room temperature.
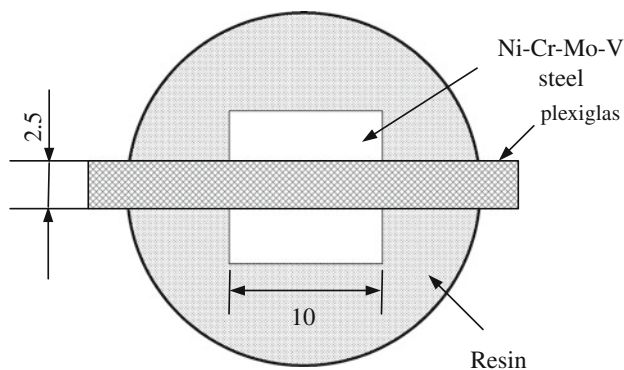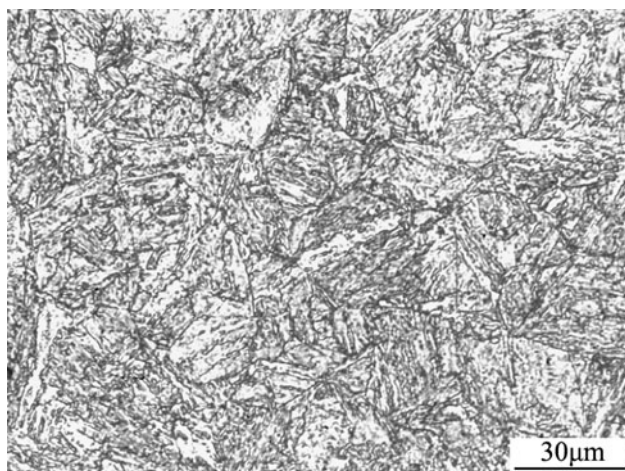
Electrochemical noise measurements were performed using an Autolab electrochemical workstation equipped with electrochemical noise (EN) module. Two identical specimens were used as the working electrode and an Ag/AgCl (saturated KCl) electrode as the reference electrode, respectively. The electrochemical current noise was measured as the galvanic coupling current between two identical working electrodes (WE) kept at the same potential. EN data were simultaneously recorded. Each set of EN records, containing 4096 data points, recorded with a data-sampling interval of 0.08 s. 127 records were analyzed for each sample. The DC trend of EN data was removed according to modified-MAR method [28].

2.3 Data analysis

Recurrence plots (RPs) are graphical tools elaborated by Eckmann et al. based on Phase Space Reconstruction [38].

Fig. 1 Schematic of the experimental setup for measuring crevice corrosion
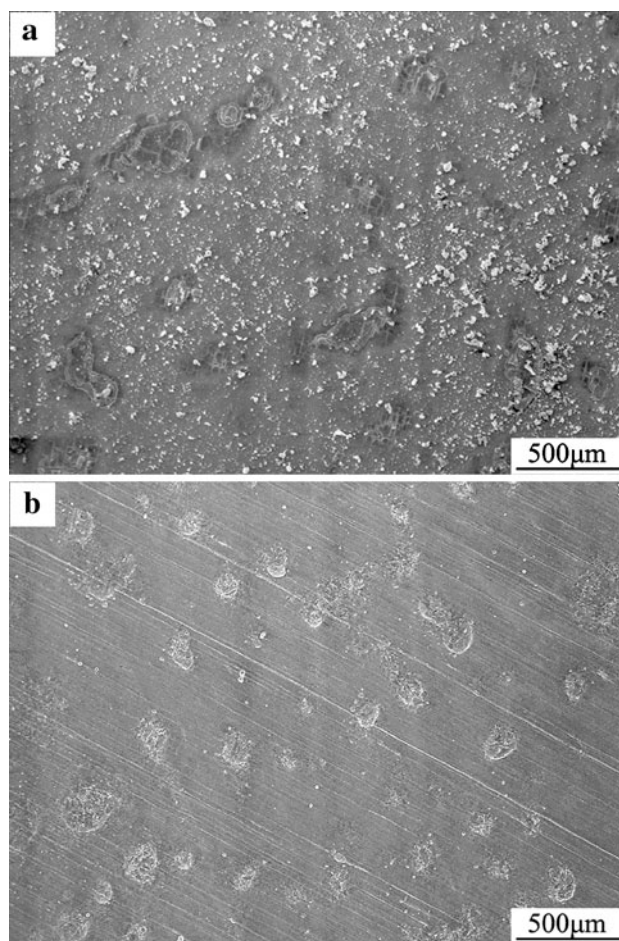

Fig. 2 Microstructure of Ni–Cr–Mo–V steel

Fig. 3 Corrosion morphology of bare Ni–Cr–Mo–V steel **a** with corrosion product, **b** without corrosion product

The method of RPs is introduced to visualize the time-dependent behavior of the dynamics of systems, which can be pictured as a trajectory in the phase space [39, 40]. It represents the recurrence of the m-dimensional phase space trajectory $\overrightarrow{x_i}$. They are a graphical representation of the $N \times N$-matrix:

$$R_{i,j} = \Theta\left(\varepsilon - \left\|\overrightarrow{x_i} - \overrightarrow{x_j}\right\|\right), \quad i,j = 1,2,3,\ldots,N,$$

where $\overrightarrow{x_i} \in R^d$ stands for the point in phase space at which the system is situated at time i, ε is a state dependent cut-off distance (a predefined threshold), $\|\bullet\|$ is the norm of vectors, $\Theta(\cdot)$ is the Heaviside function and N is the number of states.

One assigns a "black" dot to the value one and a "white" dot to the value zero. The two-dimensional graphical representation of $R_{i,j}$ then is called a RP.

There are two different types of RPs: unthresholded recurrence plots (UTRP) and thresholded recurrence plots (TRPs), respectively. An unthresholded RP is not binary but its matrix $R_{i,j}^u$ is given by the (real valued) distances of the vectors $\overrightarrow{x_i}$ and $\overrightarrow{x_j}$. The matrix is then usually represented in a two-dimensional colored plot. It has been shown that from an unthresholded RP it is possible to reconstruct time series [19]. However, unthresholded RPs are more difficult to quantify than binary RPs. For this reason, in data analysis usually binary RPs is used.

The basic idea to keep in mind when studying RPs is simple: if the underlying signal is truly random and has no structure, the distribution of colors over the RP will be uniform, and so there will not be any identifiable patterns. On the other hand, if there is some determinism in the signal generator, it can be detected by a characteristic

Fig. 4 Corrosion morphology of Ni–Cr–Mo–V steel with crevice **a** low magnification with corrosion product, center zone of covered steel **b** with corrosion product and **c** without corrosion product, boundary zone of covered steel **d** with corrosion product and **e** without corrosion product
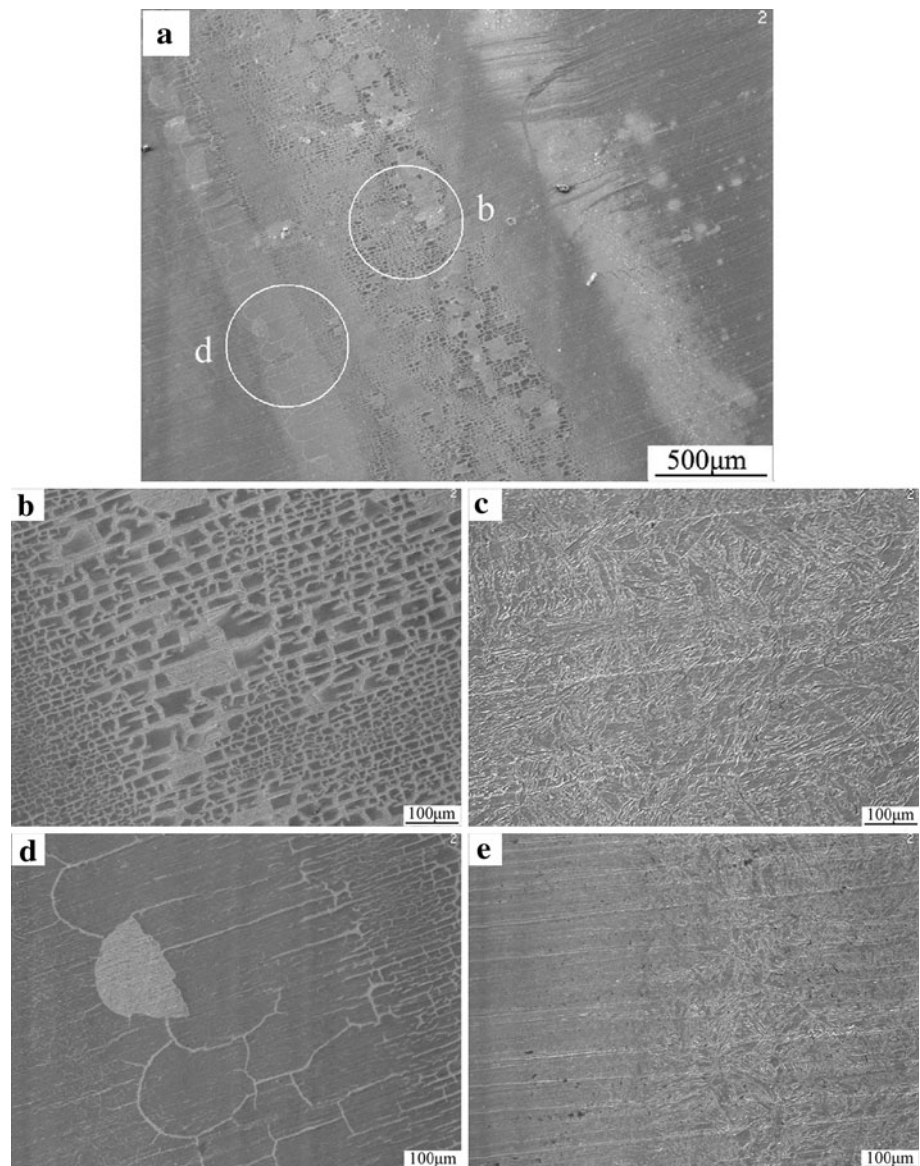
distinct distribution of colors. Considering this, the length of diagonal line segments of the same color on the UTRP can give an idea about the signal predictability. In UTRPs, hot colors (white, yellow, and orange) can be associated with small distances between vectors, while cold colors (blue, black) may be used to show large distances. In this way, it is possible to visualize and study (qualitatively) the motion of the system trajectories and infer some characteristics of the dynamical system that generated the time series.

Considering that the graphical presentation given by recurrence might be difficult to be evaluated visually, Zbilut and Webber [41] did propose a set of parameters which are part of the recurrence quantification analysis (RQA). In this work, we did consider the use of the following parameters of RQA:

The percent recurrence ($R\%$), quantifies a percentage of the plot occupied by recurrent points. It quantifies the number of time instants characterized by a recurrence in the signals interaction: the more periodic the signal dynamics, the higher the $R\%$ value.
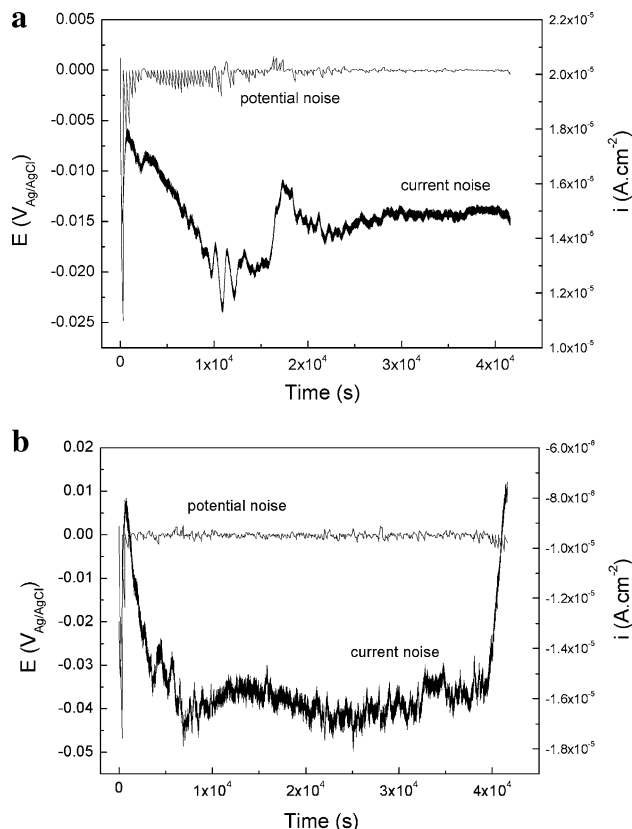
The percent determinism ($D\%$), quantifies a percentage between the recurrent points that form upward diagonal line segments and the entire set of recurrence points. The diagonal line consists of two or more points that are diagonally adjacent with no intervening white space. This parameter contains the information about the duration of a stable interaction: the longer the interactions, the higher the $D\%$ value.

The ratio is defined as: percent determinism/percent recurrence ($D\%/R\%$). The ratio represents the status change of the non-linear dynamic system.

2.4 Corrosion morphology observation

The corrosion morphologies of Ni–Cr–Mo–V steel after immersing in 3.5% NaCl solution for 12 h with and without crevice were observed by scanning electron microscope (S-400). To observe the corrosion morphology under the corrosion products, the corrosion products were removed using the chemical products-cleanup method (idt ISO 8407:1991).
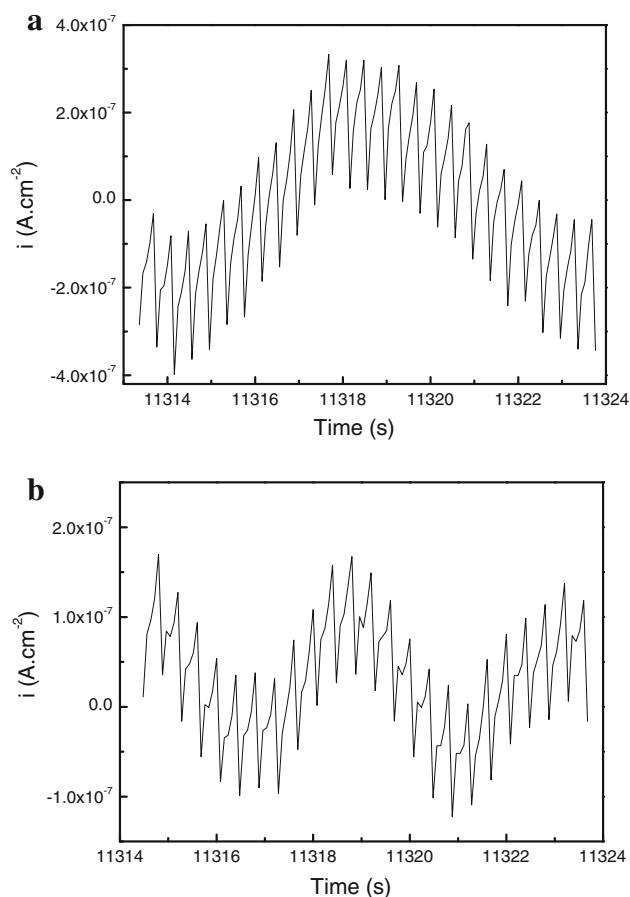

Fig. 5 The raw EN data of Ni–Cr–Mo–V steel **a** with crevice and **b** without crevice

Fig. 6 The EN transients of Ni–Cr-Mo-V steel **a** with crevice and **b** without crevice

3 Results and discussion

3.1 Corrosion morphology

After 12 h of immersion, the corrosion morphology of bare steel was shown in Fig. 3a. After the removal of corrosion product (raised by reviewer 1), shallow-disk shape localized corrosion cavities were observed, Fig. 3b.

For the steel covered by crevice, the center and the boundary zone under crevice exhibited distinguishing feature (Fig. 4a): for the center zone, a mud-cracking corrosion product with lower dimension formed on the steel surface (Fig. 4b); for the boundary zone, the cracking corrosion produce with larger dimension covered on the surface, some cracking corrosion product fall out and the corroded steel exposed (Fig. 4d). After the removal of corrosion product (raised by reviewer 1), both the center and boundary zone illustrated similar character, the covered steel showed a uniform corrosion feature (Fig. 4c, d).

3.2 EN transients and noise resistance

The electrochemical noise raw data of Ni–Cr–Mo–V steel during immersion for 12 h with and without crevice was shown in Fig. 5. In order to obtain the detail information, the representative current noise transients were illustrated in Fig. 6. For the pattern shape of transients, there was a slow stepwise rise in current from background and a fast repassivation, which indicated metastable pitting events undertook on the steel surface [42]. For the lifetime of transient, it seemed that there was no obvious discrepancy between EN data obtained from bare and crevice condition (approximately 0.4 s). However, for the height of transient, the transient height of bare sample (about 3×10^{-7} A cm^{-2}) seemed higher than that of crevice sample (around 1×10^{-7} A cm^{-2}).

The DC trend of EN data was removed according to modified-MAR method [28] and showed in Fig. 7. After DC trend removal, the EN data were analyzed.

EN data analysis in the time domain involved the calculation of the electrochemical noise resistance R_n, which was defined as the ratio of a standard deviation of the potential to that of the current noise. The value of $1/R_n$ was proportional to the corrosion rate which was calculated instantaneously [15–18]. The Fig. 8 presented $1/R_n$ of Ni–Cr–Mo–V steel with and without crevice, which indicated that three different corrosion stages were distinguished: induction stage, transformation stage, and stable stage.
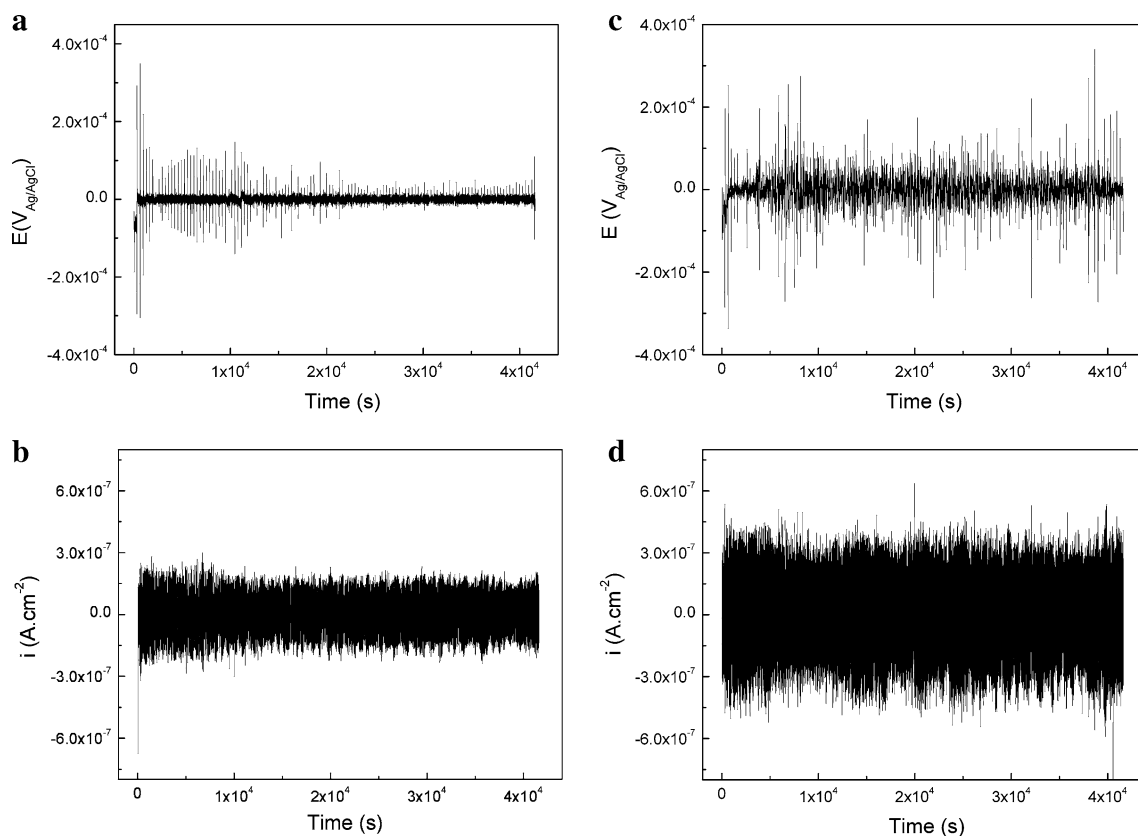

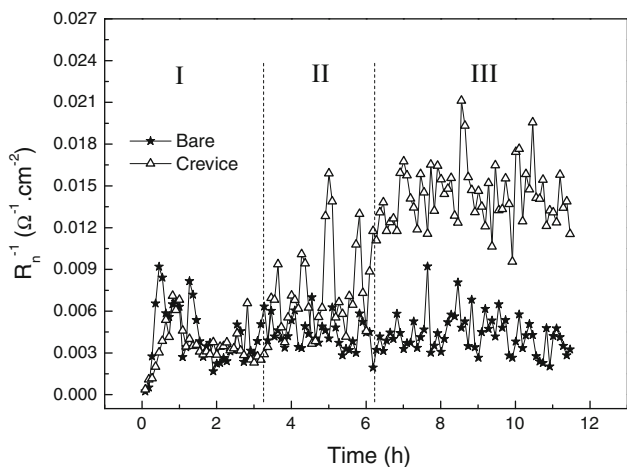Fig. 7 The EN data after DC trend removal a, b with crevice and c, d without crevice

Fig. 8 The values of $1/R_n$ of Ni–Cr–Mo–V steel with and without crevice during 12 h immersion period, *I* induction stage, *II* transformation stage, and *III* stable stage

For the induction stage of crevice corrosion (the first 3.3 h), the corrosion rate of Ni–Cr–Mo–V steel was low ($1/R_n$ was about 3.5 mΩ^{-1} cm^{-2}) and fluctuated with smaller amplitude.

For the transformation stage (when the immersion time ranged from 3.3 to 6.2 h), the corrosion rate data points deviated from the baseline and scattered with a larger amplitude fluctuations (>10 mΩ^{-1} cm^{-2}), which indicated that Ni–Cr–Mo–V steel surface was undertaking the serious metastable corrosion events.

For the stable stage of crevice corrosion (after 6.2 h of immersion), the corrosion rate of Ni–Cr–Mo–V steel remained a higher level (around 15 mΩ^{-1}cm^{-2}) and characterized by relative smaller amplitude fluctuations ($\sim$4 mΩ^{-1} cm^{-2}), which suggested that frequent corrosion events occurred on the steel surface.
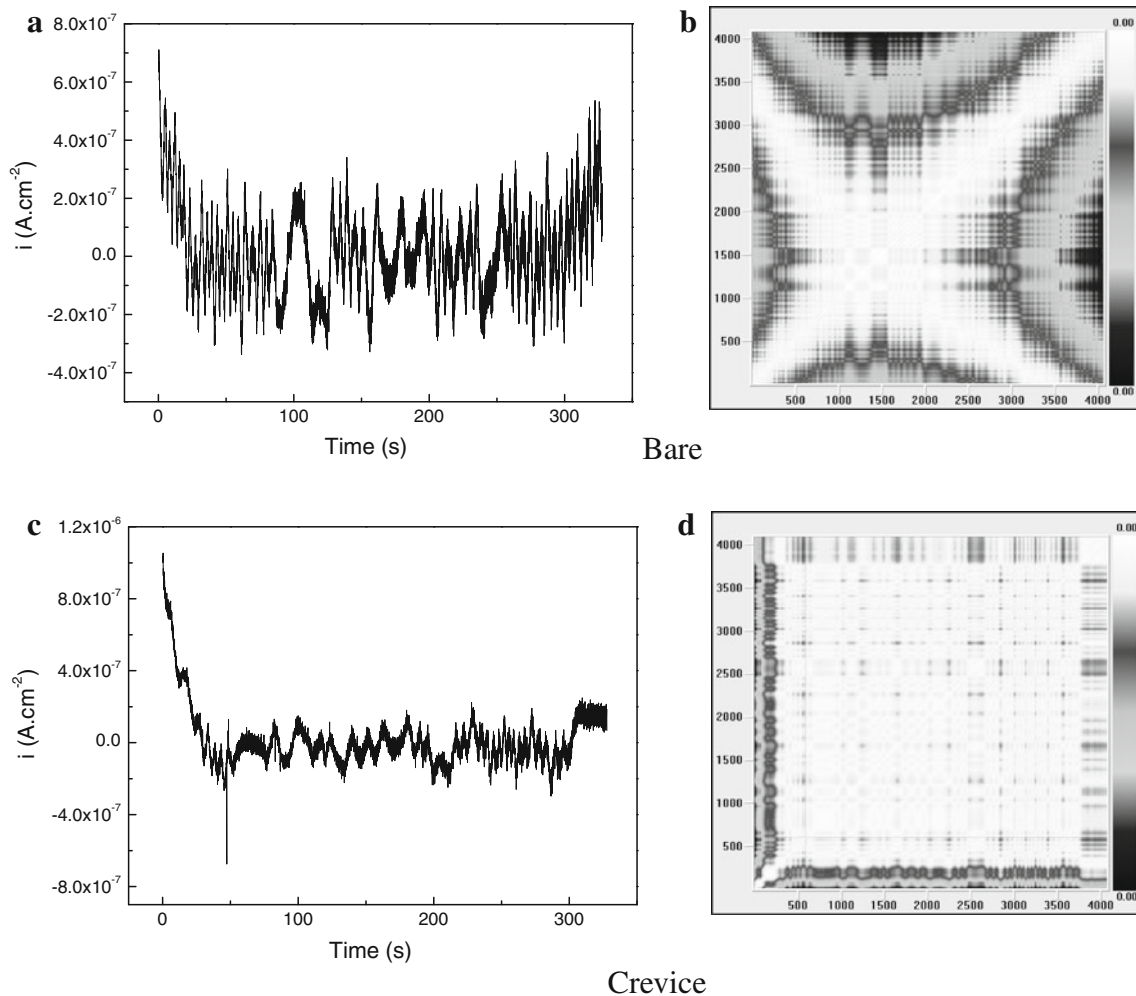

Bare

Crevice

Fig. 9 Recurrence plots obtained from current noise time series with different immersion time **a**, **b** bare, $t = 0.08$–327.68 s; **c**, **d** crevice, $t = 0.08$–327.68 s; **e**, **f** bare, $t = 11277$–11605 s; **g**, **h** crevice, $t = 38979$–39307 s; **i**, **j** bare, $t = 11277$–11605 s; **k**, **l** crevice, $t = 38979$–39307 s
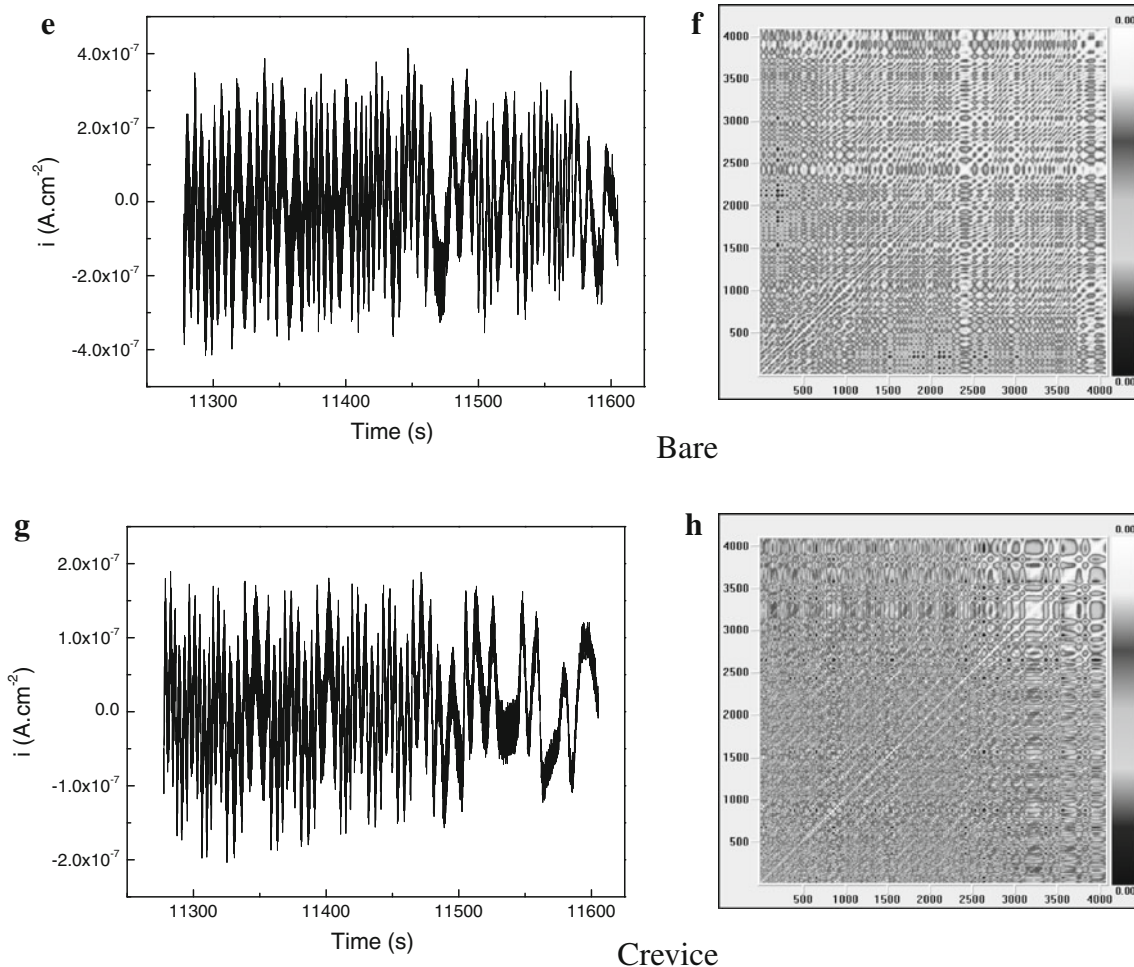
Bare

Crevice

Fig. 9 continued

3.3 Recurrence plots analysis

A collection of electrochemical noise signals with and without crevice and their respective Rps were shown in Fig. 9. All RPs were classified into categories depending upon the magnitude of the distance and color coded as follows: white and yellow pixels represent system states that are closest to each other in the reconstructed phase space, green pixels correspond to intermediate distances, while blue and black pixels represent still "recurrent states" but separated by even larger distances.

As could be observed, the crevice condition of the steel samples modifies substantially the EN signal dynamics. This was clearly shown in the structure of the RPs where the number of points of long distances (cyan and blue points) decreased in the presence of crevice, which indicated that the steel without crevice undertook localized electrochemical corrosion. In other words, corrosion occurred under the covered zone by crevice was more

uniform than that of bare sample, which was consistent with the results of the corrosion morphology.

In order to go beyond the visual notion yielded by RPs, a number of measures of complexity which quantify the small scale structures in RPs, had been proposed [39, 41] and were known as recurrence quantification analysis (RQA). Among the quantities that were usually calculated in a RQA, the following parameters were considered in thin work: percent recurrence ($R\%$), percent determinism ($D\%$) and the Ratio ($D\%/R\%$). As mentioned in the Sect. 2.3, the more periodic the transient, the higher the $R\%$ value.

The $R\%$ value of Ni–Cr–Mo–V steel with and without of crevice was evaluated and was presented in Fig. 10 as a function of the immersion time. This plot indicated that the $R\%$ value of bare sample (ranged from 0.71 to 8.19%) was higher than that with crevice (about 0.25–0.6%), which indicated that the EN transients of bare Ni–Cr–Mo–V steel were more periodic than that with crevice. Considering the features of the current noise transients (approximately
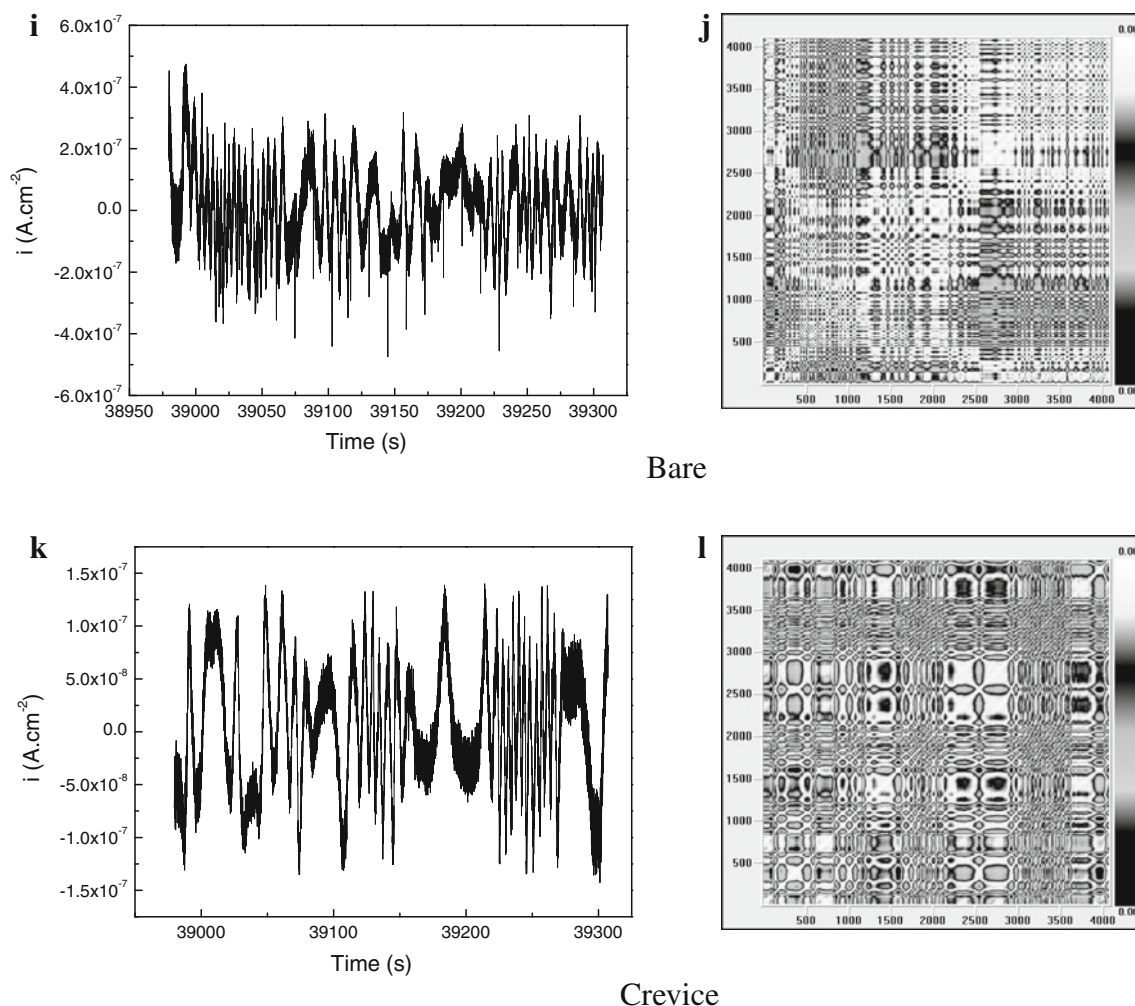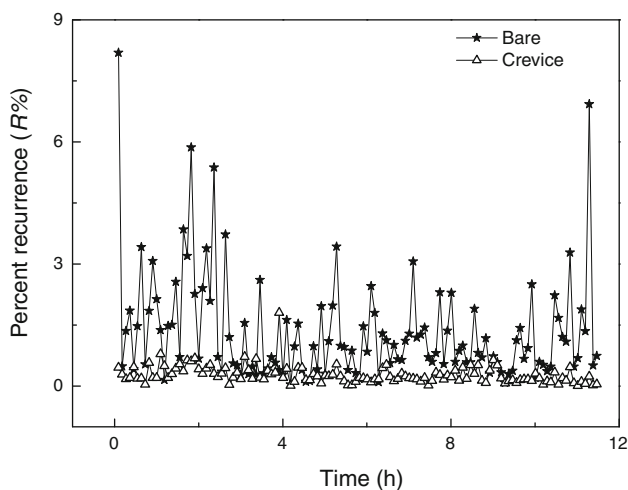
Bare

Crevice

Fig. 9 continued

Fig. 10 $R\%$ as a function of immersion time with and without crevice

equivalent transient pattern and lifetime), Fig. 6, higher periodicity of transients indicated higher generation frequency of transients. In other words, higher $R\%$ value revealed higher initiation rate of corrosion. From Fig. 10, it implied that more metastable corrosion was generated on the bare steel surface. In other words, the presence of crevice decreased the initiation rate of metastable corrosion of Ni–Cr–Mo–V steel.

The percent determinism ($D\%$), contained the information about the duration of a stable interaction: the longer the interactions, the higher the $D\%$ value. Some researchers [33–36] further revealed that higher the $D\%$ value, the higher stable localized corrosion weight of all the corrosion events occurred on the metal surface. The $D\%$ value of Ni–Cr–Mo–V steel with and without crevice was illustrated in Fig. 11. For the bare steel, $D\%$ data points remained at
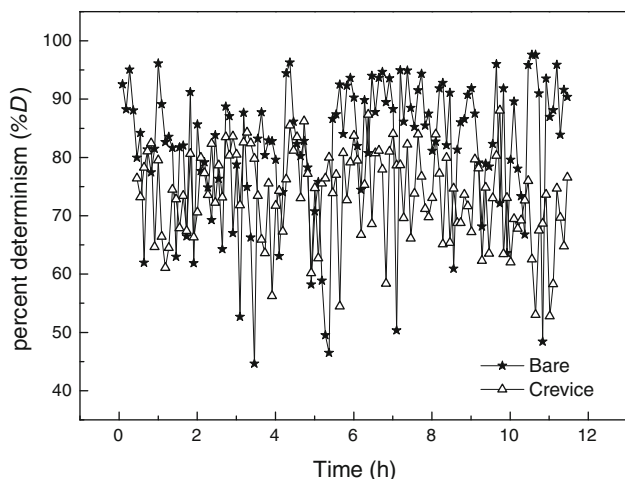
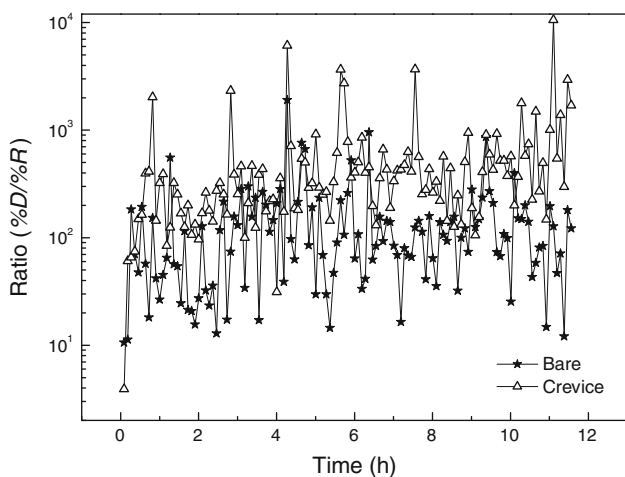**Fig. 11** *D%* as a function of immersion time with and without crevice

Fig. 12 The value of ratio as a function of immersion time with and without crevice

higher value level (approximately 81.59%); while, in the presence of crevice, the *D%* value illustrated a lower level (about 72.89%). Figure 10 indicated that the corrosion occurred on the covered Ni–Cr–Mo–V steel surface was less localized than that on bare steel surface.

The ratio was a key parameter to describe the status change of non-linear dynamic system, which is defined as: *D%/R%*. In this work, *R%* represented the initiation rate of metastable corrosion, *D%* implied stable corrosion weight of all the corrosion events; therefore, the ratio (*D%/R%*) indicated the transition of metastable corrosion to stable corrosion. To some degree, the ratio described the growth probability of metastable corrosion. Figure 12 showed the ratio value of Ni–Cr–Mo–V steel with and without crevice.

The ratio value of bare steel kept at a lower level (around 150.61). However, in the case of crevice, the ratio

value remained a higher level (about 629.37). Figure 12 revealed that the presence of crevice increased the growth probability of metastable corrosion. The metastable corrosion on Ni–Cr–Mo–V steel surface was easy to develop to stable one in the case of crevice.

4 Conclusion

The crevice corrosion behavior of Ni–Cr–Mo–V steel in NaCl solution could be divided into three stages: an induction stage, a transformation stage, and a stable development stage.

The EN results analyzed by RQA showed that the presence of crevice decreased the initiation rate of metastable corrosion, but increased the growth probability of metastable corrosion. The metastable corrosion on Ni–Cr–Mo–V steel surface was easy to develop to stable one in the case of crevice.

References

1. Oldfield J, Sutton W (1978) Br Corros J 13:13
2. Oldfield J, Sutton W (1980) Br Corros J 31:15
3. Abdulsalam M (2005) Corros Sci 1336:47
4. Brossia C, Kelly R (1998) Corros Sci 1851:40
5. Bocher F, Presuel-Moreno F, Scully J (2008) J Electrochem Soc C256:155
6. Yan M, Wang J, Han E, Ke W (2007) Corros Eng Sci Tech 42:42
7. Oldfield J, Sutton W (1978) Br Corros J 104:13
8. Zhu Y, Qiu Y, Guo X (2008) J Appl Electrochem 1017:39
9. Pickering H, Frankenthal R (1972) J Electrochem Soc 1297:119
10. Pickering H (1989) Corros Sci 325:29
11. Al-Zahrani A, Pickering H (2005) Electrochim Acta 3420:50
12. Xu Y, Wang M, Pickering H (1993) J Electrochem Soc 3448:140
13. Sawford M, Ateya B, Abdullah A, Pickering H (2002) J Electrochem Soc B198:149
14. Abdulsalam M, Pickering H (1998) J Electrochem Soc 2276:145
15. Chen J, Bogaerts W (1995) Corros Sci 1839:37
16. Lafront A, Zhang W, Jin S, Tremblay R, Dubé D, Ghali E (2005) Electrochim Acta 489:51
17. Mansfeld F, Sun Z, Hsu C (2001) Electrochim Acta 3651:46
18. Zhang T, Shao Y, Meng G, Wang F (2007) Electrochim Acta 561:53
19. Haruna T, Morikawa Y, Fujimoto S, Shibata T (2003) Corros Sci 2093:45
20. Caridade C, Isabel M, Pereira S, Brett C (2004) Electrochim Acta 785:49
21. Aballe A, Bethencourt M, Botana F, Marcos M (1999) Electrochem Commun 266:1

22. Aballe A, Bethencourt M, Botana F, Marcos M (1999) Electrochim Acta 480:44
23. Aballe A, Bethencourt M, Botana F, Marcos M, Sánchez-Amaya J (2001) Electrochim Acta 2353:46
24. Cao F, Zhang Z, Su J, Shi Y, Zhang J (2006) Electrochim Acta 1359:51
25. Zhao B, Li J, Hu R, Du R, Lin C (2007) Electrochim Acta 3976:52
26. Huang J, Guo X, Qiu Y, Chen Z (2007) Electrochim Acta 680:53
27. Zhang T, Liu X, Shao Y, Meng G, Wang F (2008) Corros Sci 3500:50
28. Liu X, Zhang T, Shao Y, Meng G, Wang F (2010) Corros Sci 892:52
29. Conde A, Williams D (1999) Mater Corros 585:50
30. Gusmano G, Marchioni F, Montesperelli G (2000) Mater Corros 537:58
31. Hu Q, Qiu Y, Guo X, Huang J (2010) Corros Sci 1205:52
32. Wharton J, Mellor B, Wood R, Smith J (2000) J Electrochem Soc 3294:147
33. Cazares-Ibáñez E, Vázquez-Coutiño G, García-Ochoa E (2005) J Electroanal Chem 317:58
34. García-Ochoa E, González-Sánchez J, Acuña N, Euan J (2009) J Appl Electrochem 637:39
35. Acuña-González N, García-Ochoa E, González-Sánchez J (2008) Int J Fatigue 1211:30
36. García E, Hernaández M, Rodríguez F, Genescá J, Boerio J (2003) Corrosion 50:59
37. ASTM Stand G48-97 (1998) Pitting and crevice corrosion resistance of stainless steel and related alloy by using ferric chloride solution. ASTM International, West Conshohocken, PA
38. Eckmann J, Kamphorst S, Ruelle D (1987) Europhys Lett 973:4
39. Zbilut J, Webber C (1992) Phys Lett A 199:171
40. McGuire G, Azar NB, Shelhamer M (1997) Phys Lett A 43:237
41. Webber CL, Zbilut JP (1994) J Appl Physiol 965:76
42. Soltis J, Krouse D, Laycock N, Zavadil K (2010) Corros Sci 838:52